Journal of Statistical Physics, Vol. 83, Nos. 1/2, 1996

Application of the Diffraction Trace Formula to the Three-Disk Scattering System

Per E. Rosenqvist,[1] Gábor Vattay,[2] and Andreas Wirzba[3]

Received January 27, 1995; final April 12, 1995

The diffraction trace formula derived previously and the spectral determinant are tested on the open three-disk scattering system. The system contains a generic and exponentially growing number of diffraction periodic orbits. In spite of this it is shown that even the scattering resonances with large imaginary part can be reproduced semiclassically. The nontrivial interplay of the diffraction periodic orbits with the usual geometrical orbits produces the fine structure of the complicated spectrum of scattering resonances, which are beyond the resolution of the conventional periodic orbit theory.

KEY WORDS: Diffraction; periodic orbits; scattering; quantum chaos.

1. INTRODUCTION

Gutzwiller's trace formula[1] is an increasingly popular tool for analyzing semiclassical behavior. Recently, it has been demonstrated that using proper mathematical apparatus, such as the spectral determinant of Voros,[2] cycle expansions,[3] or quantum Fredholm determinants,[4] the trace formula can successfully predict individual eigenenergies of bound systems and resonances of open scattering systems. The physical content of the trace formula is the geometrical optical approximation of quantum mechanics via canonical invariants of closed classical orbits. This approximation is very accurate when periodic orbits sufficiently cover the phase space of the chaotic system. This is not the case when the number of obstacles is small or their distance is large compared to their typical size. Such a problem occurs where the wavelength of a quantum mechanical (or optical) wave is very large compared to the spatial variation of a repulsive

[1] Niels Bohr Institute, DK-2100 Copenhagen, Denmark.
[2] Institute for Solid State Physics, Eötvös University, H-1088, Budapest, Hungary.
[3] Institut für Kernphysik, Technische Hochschule Darmstadt, D-64289 Darmstadt, Germany.

0022-4715/96/0400-0243$09.50/0

potential, e.g., at the boundaries of microwave guides, optical fibers, superconducting SQUIDS, or circuits in the ballistic electron transport, i.e., in most of the devices used for so-called mesoscopic physics. In such cases it is important to take into account the next-to-geometrical effects. In ref. 5 we showed how the geometric theory of diffraction (GTD) for hard-core potentials can be incorporated into the periodic orbit theory. We worked out the two-disk scattering system as an example, where diffraction plays an important role. Since the realization of the importance of such effects, diffraction periods have been uncovered in rhomboid billiards,[6] billiards with magnetic flux lines,[7] and in a limiting case of the hyperbola billiard.[8] In the present example we study for the first time a generic example where exponentially many diffractive and geometrical orbits interplay and build up a complicated spectrum of scattering resonances. For the reader unfamiliar with the diffraction trace formula we start by a brief sketch of its derivation. For a more detained and completely outlined introduction to the theory we refer the reader to ref. 9.

2. DIFFRACTION PERIODIC ORBITS

As is well known, the free-particle Green function $G(x, y; E)$ can be exactly described in terms of geometrical optics by the path that connects x with y at energy E. If a smooth potential is introduced, we have to respond with a refractive index and if hard walls are present, we have to deal with diffractive rays to keep the description in the spirit of geometrical optics. The diffractive rays connecting two points in the configuration space can be derived from an extension of Fermat's variational principle of classical mechanics: Each path connecting x with y has a whole class of topologically equivalent paths which can all be continuously deformed into each other without changing the number of encounters with the hard-wall singularities of the system. The generalized Fermat principle then states that for each such class Γ only the rays of stationary optical length among all the curves in Γ contribute to the final field. The total field will then be the sum of contributions from such paths with diffractive segments, over all the topologicaly different classes of paths connecting x with y.

Once we know the generalized ray connecting two points $\mathscr{A}$ and $\mathscr{B}$, we can compute semiclassicaly the Green function $G(q_{\mathscr{A}}, q_{\mathscr{B}}, E)$ by tracing the ray:[10]

a. On the geometrical segments of the ray, the Green function is given by the energy-domain Van Vleck propagator

$$G(q, q', E) = \frac{2\pi}{(2\pi i\hbar)^{3/2}} D_V^{1/2}(q, q', E) \exp\left[\frac{i}{\hbar} S(q, q', E) - \frac{i}{2} \nu\pi\right] \qquad (1)$$

where

$$D_\nu(q, q', E) = |\det(-\partial^2 S/\partial q_i \partial q'_j)|/|\dot{q}| \cdot |\dot{q}'|$$

is the Van Vleck determinant and ν is the Maslov index (see ref. 11 for details).

b. When the geometrical ray hits a surface, an edge, or a vertex of the obstacle it creates a source for the diffracted wave. The strength of the source is proportional to the Green function at the incidence of the ray

$$Q_{\text{diff}} = DG_{\text{inci}} \tag{2}$$

The diffraction constant D depends on the local geometry of the obstacle, the wave-type, and the nature of the diffraction. It has been determined in ref. 10 from the asymptotic semiclassical expansion of the exact solution in a simple geometry, namely the scattering from a single disk.[10, 12] For the surface diffraction (creeping) it has the form

$$D_l = 2^{1/3} 3^{-2/3} \pi e^{5i\pi/12} \frac{(k\rho)^{1/6}}{Ai'(x_l)} \tag{3}$$

Here $Ai'(x)$ is the derivative of the Airy integral $Ai(x) = \int_0^\infty dt \cos(xt - t^3)$, $k = (2mE)^{1/2}/\hbar$ is the wave number, ρ is the radius of the obstacle at the source of the creeping ray, and x_l are the zeros of the Airy integral. The index $l \geqslant 1$ refers to the possibility of initiating creeping rays with different modes, each with its own profile. In practice, only the low modes contribute to the Green function. For wedge diffraction the diffraction constant is

$$D_{\text{wedge}} = \frac{\sin(\pi/n)}{n} \left[\frac{1}{\cos(\pi/n) - \cos[(\theta - \alpha)/n)]} - \frac{1}{\cos(\pi/n) - \cos[(\theta + \alpha + \pi)/n]} \right] \tag{4}$$

where $(2-n)\pi$ is the angle of the wedge (n is a real number), α is the incident angle, and θ is the outgoing angle. For details we refer to ref. 10. In the three-disk scatterer the wedge diffraction is only important when the system is closed, and we shall therefore not go deeper into the subject here.

The source created by the incident ray then initiates a new ray propagating along the surface (for creeping) or a free ray starting at the edge of the obstacle (wedge diffraction).

During the creeping of the ray the amplitude decreases, which can be understood as a process analogous to the radiation processes of electrodynamics. The radiated intensity is proportional to the intensity of the ray

$$\frac{d}{ds} A_l(s, E)^2 = -2\alpha_l(s, E)\, A_l(s, E)^2 \tag{5}$$

where s is the length measured along the surface and $A_l(s, E)$ is the complex amplitude of the Green function along the surface. The coefficient $\alpha_l(s, E)$ depends on the local curvature of the surface, $1/\rho(s)$, and it has the structure $\alpha_l(s, E) = x_l e^{-i\pi/6}[k/6\rho(s)^2]^{1/3}$ (see ref. 13), where the index l refers again to the different modes of the creeping wave. The Green function for the creeping ray of mode l is then given by

$$G_l^D(q_{\mathscr{A}'}, q_{\mathscr{B}'}, E) = \exp\left[-\int_0^L ds\, \alpha_l(s, E)\right] \exp\left[\frac{i}{h} S(q_{\mathscr{A}'}, q_{\mathscr{B}'}, E)\right] \tag{6}$$

where L is the length of the arc of the creeping ray, and $S(q_{\mathscr{A}'}, q_{\mathscr{B}'}, E)$ is the action along it.

When the creeping ray leaves the surface its intensity can be calculated from the relation (2) due to the reversibility of the Green function. The total Green function is then the *product* of the Green functions and diffraction coefficients along the ray. If, for example, we have geometrical propagation from $\mathscr{A}$ to $\mathscr{A}'$followed by surface creeping from $\mathscr{A}'$ to $\mathscr{B}'$ and then again a geometrical propagation from $\mathscr{B}'$ to $\mathscr{B}$, the total semiclassical Green function is

$$G(q_{\mathscr{A}}, q_{\mathscr{B}}) = G(q_{\mathscr{A}}, q_{\mathscr{A}'})\, D_{\mathscr{A}'} G^{Cr}(q_{\mathscr{A}'}, q_{\mathscr{B}'})\, D_{\mathscr{B}'} G(q_{\mathscr{B}'}, q_{\mathscr{B}}) \tag{7}$$

Corrections to this formula result from h contributions to the geometrical legs and polynomial Airy corrections to the creeping arcs. In case we have geometrical propagation from $\mathscr{A}$ to $\mathscr{A}'$ followed by a wedge diffraction and finally again a geometrical propagation from $\mathscr{A}'$ to $\mathscr{B}$, the total semiclassical Green function reads

$$G(q_{\mathscr{A}}, g_{\mathscr{B}}) = G(q_{\mathscr{A}}, q_{\mathscr{A}'})\, D_{\text{wedge}} G(q_{\mathscr{A}'}, q_{\mathscr{B}}) \tag{8}$$

Contrary to the pure geometrical case, the semiclassical energy-domain Green function for rays with diffraction arcs or wedge diffraction thus has a *multiplicative* composition law.

When we incorporate diffraction effects into the trace formula, periodic rays with diffraction segments also contribute. We can handle separately the pure geometric cycles and the cycles with at least one diffraction arc or wedge:

$$\operatorname{Tr} G(E) \approx \operatorname{Tr} G_G(E) + \operatorname{Tr} G_D(E) \tag{9}$$

where $\operatorname{Tr} G_G(E)$ is the ordinary Gutzwiller trace formula, while $\operatorname{Tr} G_D(E)$ is the new trace formula corresponding to the nontrivial cycles of the GTD. The Gutzwiller trace formula for two-dimensional billiards is

$$\operatorname{Tr} G_G(E) = \frac{1}{ih} \sum_p \sum_{r=1}^{\infty} T_p(E) \frac{\exp[irS_p(E) - irv_p\pi/2]}{|\Lambda_p^r|^{1/2}(1 - 1/\Lambda_p^r)} \tag{10}$$

where $T_p(E)$ is the time, $S_p(E)$ is the classical action, v_p is the Maslov index, and Λ_p is the stability eigenvalue of the primitive periodic orbit. The summation goes for all primitive periodic orbits of the system p and their repetitions r. The $\operatorname{Tr} G_D(E)$ can be computed by using appropriate Watson contour integrals.[12] For technical details we refer the reader to refs. 12 and 14. If we denote by q_i, $i = 1,\ldots, n_p$ (with $q_{n_p+i} \equiv q_i$), the points along the closed cycle where the ray changes from diffraction to pure geometric evolution or vice versa or where the ray encounters a wedge diffraction, the trace for cycles with *at least one diffraction arc* can be expressed as the product

$$\operatorname{Tr} G_D(E) = \frac{1}{ih} \sum_p \sum_{r=1}^{\infty} T_p(E) \prod_{i=1}^{n_p} [D(q_i)\, G(q_i, q_{i+1}, E)]^r \tag{11}$$

where $T_p(E)$ is the time period of the primitive cycle and $D(q_i)$ is the diffraction constant (3) or (4) at the point q_i. Here $G(q_i, q_{i+1}, E)$ is either the Van Vleck propagator if q_i and q_{i+1} are connected by pure geometric arcs or is given by the creeping propagator (6) in case q_i and q_{i+1} are the boundary points of a creeping arc.

3. THE THREE-DISK SYSTEM

To investigate the theory sketched above, we apply it to the three-disk scattering system. The three-disk system has in recent years been subjected to a large number of investigations, and its main virtues are well known. Here, we recall some of the basic properties of the system.

The system consists of three identical disks placed symmetrically around the origin in a plane (see Fig. 1), and is completely determined by

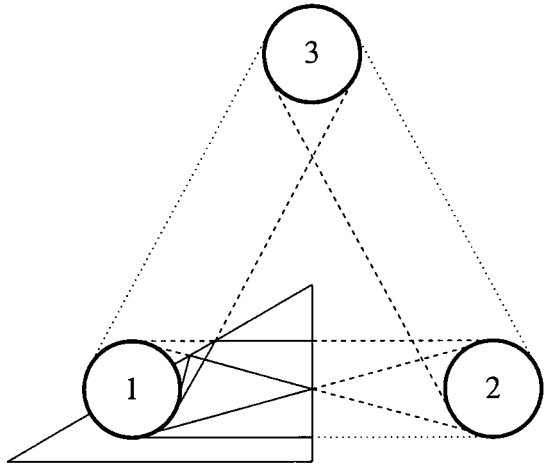

Fig. 1. The full three-disk system with a copy of the fundamental domain. Representatives of the creeping orbits of topological length 1 are displayed in full space as well in the fundamental one.

a single parameter, namely the ratio $R:a$ of the separation of the disks to their radius. In our calculations we have kept this ratio fixed at $R:a=6$.

The system thus possesses a threefold rotational symmetry around the origin and has three reflection symmetries around the symmetry lines through the center. The system is therefore invariant under the point group C_{3v}; instead of considering the system as a whole, we can restrict ourselves to the *fundamental domain*.[15] The fundamental domain exactly covers the whole system when the elements of the point group are applyed to it. The three-disk system and a version of the fundamental domain are shown in Fig. 1. For sufficiently large spacing of the disks[17] the system has a complete binary symbolic dynamics. All the periodic orbits can be described in terms of the alphabet $\{0, 1\}$, where 0 corresponds to a bounce under which the particle returns to its starting disk and 1 corresponds to the bounces where the particle continues to the next disk. In the fundamental domain there are therefore two fixpoints 1 and 0 corresponding to a triangular and back-and-forward bouncing orbit in the full space. All the geometrical orbits can be found via a minimization of the path lengths. If one needs a periodic orbit following a definite sequence of n disk bounces, one just has to determine the length as a function of the n bouncing positions and then to minimize this length. That this indeed gives the right periodic orbit follows from geometrical optics and Fermat's principle: when the light (the particle) follows the shortest path (of a given symbolic sequence), it will at the same time obey the reflection law.

The surface of the disk in the fundamental domain can be used as a Poincaré surface of section. Establishing the bouncing map as in ref. 18, we can thus calculate the stabilities of the cycles. Following the outlined scheme, we arrive at the results displayed in Table I.

A more detailed description of the three-disk system and the methods described in this section can be found in, e.g., ref. 18.

In order to apply the GTD to the calculation of semiclassical resonances, we also have to account for the diffraction (creeping) orbits of the system. To give an overview of the work to be done, we start by counting the number of periodic creeping orbits to be evaluated. Because of the symmetry of the system we can assume that the creeping orbit always starts tangentially from the (half-) disk in the fundamental domain which we label disk number 1. Considering first an orbit with no geometrical bounces, we see that it has two different disks to go to, and for each each disk two different sides to creep in. This makes a total of four diffraction orbits of topological length 1. When these are folded back into the fundamental domain we see that two of them are self-retracing. The two other orbits are tracing the same orbit, but in opposite directions. If we

Table I. Geometrical Cycle Data for the Three-Disk System with $R:a=6$[a]

p	Λ_p	L_p^G/a
0	9.898979	4.000000
1	−11.771455	4.267949
10	−124.094801	8.316529
100	−1240.542557	12.321746
101	1449.545074	12.580807
1000	−12295.706861	16.322276
1001	14459.975919	16.585242
1011	−17079.019008	16.849071
10000	−121733.838705	20.322330
10001	143282.095154	20.585689
10010	153925.790742	20.638238
10011	−170410.715542	20.853571
10101	−179901.947942	20.897369
10111	201024.734743	21.116994

[a] The first column indicates the symbolic dynamics of the periodic orbit, and the second and third column gives the stability calculated from the Jacobian of the bouncing map and the length of the cycle in the fundamental domain, respectively.

consider paths of the particle with m bounces, we see that there will be $2^{n+1}=2^{m+2}$ periodic creeping orbits of topological order n, as for each one of the m bounces the particle can choose between two disks. Thus the number of periodic creeping orbits grows exponentially fast with the topological length n of the orbit. It is quite astonishing, however, as we will see later, how few of these orbits are in fact needed to get a good description of the scattering resonances (including the ones with large imaginary parts). The creeping orbits can be described completely by their itinerary $1\alpha_1\alpha_2\cdots\alpha_n$, where the α_i are taken from the alphabet $\{1, 2, 3\}$ and where we do not allow the repeats $\cdots 11\cdots 22\cdots$, and $\cdots 33\cdots$. This description contains a double degeneracy due to the fact that the orbit has the choice to creep around the final disk clockwise or anticlockwise. For instance, 123 can represent two different orbits which start from disk 1 in the fundamental domain, then hit disk number 2, and finally creep around the final disk (3) clockwise or anticlockwise.

The restriction that the creeping periodic orbits should start and end tangentially on one of the disks simplifies the search procedure for them considerably: whereas in the case of geometrical n-bounce cycles one had to minimize a function of n bouncing parameters, we here only have one parameter in play, namely the angle where the creeping orbit leaves the initial disk. Suppose now that we want a specific creeping orbit described by a series of disk bounces plus the specification of the final creeping domain as above. We then scan through all the angles that leave the first disk in the fundamental domain. This gives us an interval of angles where the first wanted disk is being hit. We then scan this interval for bounces on the next disk in tire itinerary axed so on. Finally, we scan the last obtained interval to find the angle under which the ray creeps into the wanted side of the final disk.

4. CYCLE EXPANSION OF THE SPECTRAL DETERMINANT

Having established the data material for the three-disk system as described above, we now report on the more technical part of the actual calculation.

The resonances can be recovered from the Gutzwiller–Voros spectral determinant $\Delta(E)$,[2] which is related to the trace formula as

$$\operatorname{Tr} G(E)=\frac{d}{dE}\ln \Delta(E) \tag{12}$$

The full semiclassical determinant can be written as the *formal* product of two spectral determinants, one corresponding to the pure geometrical, and

one to the new diffractional cycles: $\Delta(E) = \Delta_G(E)\,\Delta_D(E)$, due to the additivity of the traces. The product is only formal since the eigenenergies are not given by the zeros of $\Delta_G(E)$ or $\Delta_D(E)$ individually, but have to be calculated from a curvature expansion of the *combined* determinant $\Delta(E)$ itself.

The geometrical part of the spectral determinant is given by

$$\Delta_G(E) = \exp\left(-\sum_p \sum_{r=1}^{\infty} \frac{1}{r} \frac{\exp[irS_p(E) - irv_p\pi/2]}{|\Lambda_p^r|^{1/2}(1 - 1/\Lambda_p^r)} \right) \tag{13}$$

where the summations are over closed primitive (nonrepeating) cycles p and their repetitions r. The diffraction part of the spectral determinant is

$$\Delta_D(E) = \exp\left(-\sum_p \sum_{r=1}^{\infty} \frac{1}{r} \prod_{i=1}^{n_p} [D(q_i^p)\, G(q_i^p, q_{i+1}^p, E)]^r \right) \tag{14}$$

where the summations are over closed primitive (nonrepeating) cycles p and their repetitions r. The product of Green functions should be evaluated for q_i^p belonging to the primitive cycle p. After summation over r, the spectral determinant can be written as

$$\Delta_D(E) = \prod_p (1 - t_p) \tag{15}$$

with

$$t_p = \prod_{i=1}^{n_p} D(q_i^p)\, G(q_i^p, q_{i+1}^p, E) \tag{16}$$

where q_i^p belongs to the primitive cycle p. Here the mode numbers l of the diffraction constants and the corresponding summations have been supressed for notational simplicity.

We can conclude that the diffractional part $\Delta_D(E)$ of the spectral determinant shares some nice features of the periodic orbit expansion of the dynamical zeta functions,[16] and it can be expanded as

$$\Delta_D(E) = 1 - \sum_p t_p + \sum_{p,p'} t_p t_{p'} - \cdots \tag{17}$$

The weight (16) has the following property, which helps in radically reducing the number of relevant contributions to the expansion: If two different cycles p and p' have at least one common piece in their diffraction arcs, then the two cycles—to leading order $l = 1$—can be combined, to one

longer cycle $p+p'$ and the weight corresponding to this longer cycle is the product of the weights of the short cycles

$$t_{p+p'} = t_p \cdot t_{p'} \tag{18}$$

As a consequence, the product of primitive cycles which have at least one common piece in their diffraction arcs can be reduced in such a way that the composite cycles are exactly cancelled in the curvature expansion

$$\prod_p (1 - t_p) = 1 - \sum_b t_b \tag{19}$$

where t_b are *basic* primitive orbits which cannot be composed from shorter primitive orbits. In the case of the desymmetrized three-disk scatterer this applies to all the orbits, and we thus get a zeta function exactly of the form (19), where the sum is over all the prime periodic creeping orbits.

To get the free-flight part of $\Delta_D(E)$ we first consider the semiclassical Green function in free space. This is asymptotically ($kR \gg 1$) given as

$$G_0(q, q', E) = -\frac{i}{4}\left(\frac{2}{\pi kR}\right)^{1/2} e^{ikR - i(\pi/4)} \tag{20}$$

where $R = |q - q'|$. If the ray connecting q and q' is reflected once or more from the curved hard walls before hitting tangentially one of the surfaces, we can keep track of the change in the amplitude by the help of the Sinai–Bunimovich curvatures. For a free flight the Sinai–Bunimovich curvature is just the inverse of the traveled distance

$$\kappa = \frac{1}{r} \tag{21}$$

When a hard wall is encountered tine curvature changes discontinuously as

$$\kappa_+ = \kappa_- + \frac{2c}{\cos\phi} \tag{22}$$

where $\kappa_\pm$ are the Sinai–Bunimovich curvatures right after and before the bounce against the wall and c is the curvature of the reflecting surface at the point of incidence, whereas ϕ is the angle of incidence.

By computing the curvatures κ_i right after the reflections and knowing the distances l_i between the ith and the $(i+1)$th points of reflections, we has to change the factor R in the Green function (20) to the effective radius $R^{\text{eff}} = l_0 \prod_{i=1}^{m} (1 + l_i \kappa_i)$ where l_0, is the distance between q and the first

point of reflection along the ray as measured from q, and m is the number of reflections from the hard potential walls. The effective radius R_b^{eff}, the length of the geometrical arc L_b^G, and the length of the diffraction part L_b^D of the first twelve orbits with creeping sections are listed in Table II. To each cycle in the list, there is a whole sequence of cycles which wind around the disk m_W times. For these orbits one has to add $2\pi a m_W$ to the diffraction length L_b^D. The diffraction part of the spectral determinant is finally given by

$$\Delta_D(k) = 1 - \sum_b (-1)^{m_b} C_l \frac{a^{1/3} \exp(i\pi/12) \exp[ik(L_b^G + L_b^D) - \alpha_l L_b^D]}{k^{1/6}(R_b^{\text{eff}})^{1/2}} \times \frac{1}{1 - \exp[2\pi(ik - \alpha_l)a]}\Bigg|_{l=1} \tag{23}$$

where $C_l = \pi^{3/2} 3^{-4/3} 2^{-5/6} / Ai'(x_l)^2$, α_l is the creeping exponent, and m_b is the number of reflections of orbit b from the disk in the fundamental domain. The summation for the windings m_W gives the factor $1/(1 - \exp[2\pi(ik - \alpha_l)a])$.

Table II. Creeping Cycle Data for the Three-Disk System with $R:a = 6$[a]

p_c	R_b^{eff}/a	L_b^G/a	L_b^D/a
12	6.000000	6.000000	4.188790
12	5.656854	5.656854	3.821266
13	6.000000	6.000000	2.094395
13	5.656854	5.656854	3.821266
121	58.167840	9.832159	4.523686
121	58.787753	9.797958	3.544308
131	58.167840	9.832159	2.429291
131	58.787753	9.797958	3.544308
123	66.352162	10.120809	4.384819
123	73.492203	10.147842	3.478142
132	84.855171	10.120809	2.678761
132	73.492203	10.147842	3.478142

[a] The first column indicates the itinerary of the orbit, the second column the effective radius of the orbit calculated by means of the Sinai–Bunimovich curvatures, and the third and fourth columns the lengths of the free-flight and the creeping sections, respectively.

5. NUMERICAL RESULTS AND CONCLUSIONS

To evaluate the results of the diffraction extended Gutzwiller–Voros spectral determinant, we compare the resonances determined by this to the resonances determined just from geometrical orbits and to the exact quantum resonances.

The data are displayed in Fig. 2 and 3. As one can see, the Gutzwiller–Voros determinant accounts reasonably well for the leading order of resonances, whereas it fails for the next series. In Fig. 3, however, we can see that—when a few periodic creeping orbits are introduced—the results are *qualitatively different*, and represent much better the trend of the exact quantum resonance data. For instance, one can make a one-to-one identification of the quantum and semiclassical resonances, which is not possible in the purely geometrical theory, since in that approximation even the number of resonances is wrong.

The series of subleading resonances also approximately defines the lower boundary of the region in which the diffractional spectral determinant still has a high accuracy and good convergence properties. This can also be seen from Fig. 3, since for small Re k and large negative Im k we have a relatively larger deviation between the exact and creeping resonances.

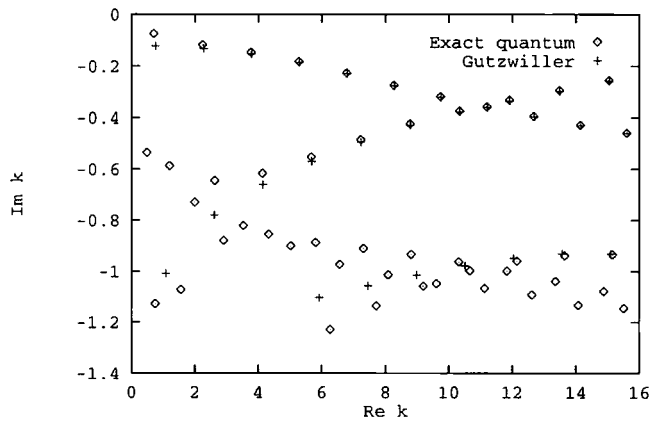

Fig. 2. The exact quantum mechanical resonances (diamonds) and the pure geometrical Gutzwiller–Voros resonances (crosses) in units of $1/a$ in the complex k plane. The resonances belong to the one-dimensional A_1 representation of the three-disk system with $R:a=6$. In the semiclassical calculation cycles up to topological length 4 have been used. The leading resonances close to the real axis are exactly described by the Gutzwiller–Voros resonances, whereas the subleading semiclassical resonances clearly deviate from the exact quantum resonances.

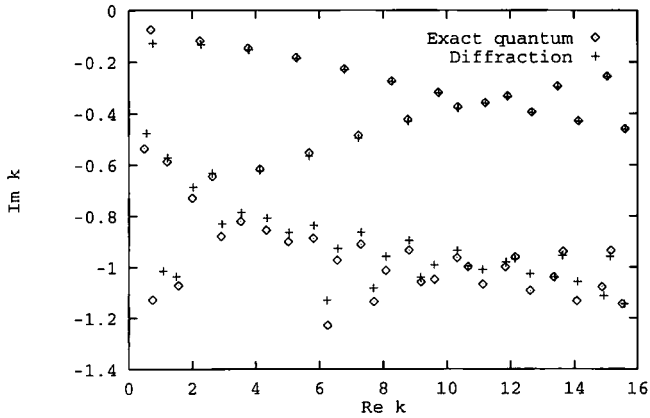

Fig. 3. The exact quantum mechanical (diamonds) and the semiclassical (crosses) A_1 resonances of the $R{:}a=6$ three-disk system. The resonances are calculated by including diffractional creeping orbits up to order four in the GTD. As in the two-disk case, an improvement of the approximation is clearly visible, especially for the second row of the leading resonances as well as for the subleading diffractional ones. In the latter case the qualitative trend is clearly reproduced. As discussed above, the accuracy of the semiclassical resonances become worse in the region where Re k is small and Im k is large.

The errors of the resonances originated from three sources.

1. The description is semiclassical and therefore we use the Van Vleck propagator in (18) instead of the exact progrator, and the semiclassical approximation of the creeping propagator in (5). In particular the polynomial terms in the Airy expansion of the creeping propagator give sizable corrections, as can be shown in the simpler one-disk and two-disk problems.[19, 20] Also, only the $l=1$ creeping modes are used.

2. Only a restricted number of usual and creeping periodic orbits is avaliable instead of infinitely many.

3. Even the cumulant expansion of the exact quantum mechanical scattering determinant is for large negative Im k very delicate as the single terms entering the cumulant expansion become individually large.[20] As the periodic orbit expansion is just the semiclassical approximation to the cumulant expansion,[14] it cannot be expected that the periodic orbit expansion works better than this. In fact, as the individual contributions of the periodic orbits become larger with increasing negative Im k, and the individual errors from the semiclassical expansion are also increasing such that the total error can become sizable. In the simpler one-disk[19] and two-disk[20] problems the contributions resulting from the higher polynomial terms in the Airy expansion of the creeping propagator move the subleading semiclassical resonances on top of their corresponding exact

quantum analogs to figure accuracy. In the three-disk case the corresponding calculation is plagued by the exponentially proliferating number of periodic orbits, but the hope is of course that the corresponding Airy correction terms could improve the subheading semiclassical resonances as well.

As mentioned earlier, the number of creeping periodic orbits in this system increases exponentially with the topological length of the cycles. It would be natural to expect that this might destroy the simplicity of the semiclassical description. We conclude that this seems not to be the case. As we have demonstrated, one only needs the basic representatives of the creeping families to change the picture of the scattering resonances drastically in the direction of the exact quantum resonances.

ACKNOWLEDGEMENT

The authors are very grateful to P. Cvitanović and P. Szépfalusy for encouragement, and A. Shudo, Y. Shimizu, N. Whelan, and S. M. Riemann for communicating their results prior to publication. P.E.R. and G.V. thank the Danish Science Foundation (SNF) for support and G.V. acknowledges the support of the Foundation for Hungarian Higher Education and Research and the Hungarian Science Foundation (OTKA 2090 and F4286).

REFERENCES

1. M. C. Gutzwiller, *J. Math. Phys.* **12**:343 (1971).
2. A. Voros, *J. Phys. A* **21**:685 (1988).
3. P. Cvitanović and B. Eckhardt, *Phys. Rev. Lett.* **63**:823 (1989).
4. P. Cvitanović and P. E. Rosenqvist, *Conference Proceedings*, Vol. 41, G. F. Dell'Antonio, S. Fantoni, and V. R. Manfredi, eds. (IPS, Bologna, 1993); P. Cvitanović and G. Vattay, *Phys. Rev. Lett.* **71**:4138 (1993); P. Cvitanović, P. E. Rosenqvist, G. Vattay, and H. H. Rugh, *Chaos* **3**(4):619 (1993); G. Vattay, *Prog. Theor. Phys. Suppl.* **116**:251 (1994).
5. G. Vattay, A. Wirzba, and P. E. Rosenqvist, Periodic orbit theory of diffraction, *Phys. Rev. Lett.* **73**:2304 (1994); Inclusion of diffration effects in the Gutzwiller trace formula, in *Proceedings of the ICDC Tokyo*, in press.
6. Y. Shimizu and A. Shudo, Preprint (1994).
7. S. M. Riemann, M. Brack, A. G. Magner, and M. V. N. Murthy, Applications of classical periodic orbit theory to circular billards with small scattering centres, Preprint.
8. N. Whelan, *Phys. Rev. E.* (April 1995).
9. G. Vattay, A. Wirzba, and P. E. Rosenqvist, In preparation.
10. J. B. Keller, *J. Opt. Soc. Am.* **52**:116 (1962); J. B. Keller, in *Calculus of Variations and its Application* (American Mathematical Society, Providence, Rhode Island, 1958), p. 27; B. R. Levy and J. B. Keller, Comm, *Commun. Pure Appl. Math.* **XII**:159 (1959); B. R. Levy and J. B. Keller, *Can. J. Phys.* **38**:128 (1960).
11. M. C. Gutzwiller, *Chaos in Classical and Quantum Mechanics* (Springer-Verlag, New York, 1990).

12. W. Franz, *Theorie der Beugung Elektromagnetischer Wellen* (Springer-Verlag, Berlin, 1957); *Z. Naturforsch.* **9a**:705 (1954).
13. B. Schrempp and F. Schrempp, *Nucl. Phys. B* **163**:397 (1980).
14. A. Wirzba, *Chaos* **2**:77 (1992); *Nucl. Phys. A* **560**:136 (1993).
15. P. Cvitanović and B. Eckhardt, Symmetry decomposition of chaotic dynamics, *Nonlinearity* **6**:277–311 (1993).
16. R. Artuso, E. Aurell, and P. Cvitanović, Recycling of strange sets, *Nonlinearity* **3**:325 (1990); **3**:361 (1990).
17. K. Hansen, Ph.D. Thesis, University of Oslo (1993).
18. P. Cvitanović, B. Eckhardt, G. Russberg, P. E. Rosenqvist, and P. Scherer, Pinball scattering, in *Quantum Chaos*, G. Casati and B. Chirikov, eds., (Cambridge University Press, Cambridge, 1994).
19. W. Franz and R. Galle, *Z. Naturforsch.* **10a**:374 (1955).
20. A. Wirzba, In preparation.